Sound & Vibration 2026, 60(3), 4216.
doi: https://doi.org/10.59400/sv4216

Article

High-precision blasting vibration prediction model integrating Bayesian theory and dimensional analysis

Bei Jia[1,2,*], Xiao Wang[3], Zhongyu Lv[1,2], Zanmin Xiong[1,2], Lulu Qi[1,2]

[1] China ENFI Engineering Corporation, Beijing 100038, China

[2] Key Laboratory of Ground Control Management Plan in Deep Metal Mines, National Mine Safety Administration, Beijing 100038, China

[3] School of Mechanics and Civil Engineering, China University of Mining Technology, Beijing 100083, China

*** Corresponding author:** Bei Jia, jiab@enfi.com.cn

CITATION

Jia B, Wang X, Lv Z, et al. High-precision blasting vibration prediction model integrating Bayesian theory and dimensional analysis. Sound & Vibration. 2026; 60(3): 4216. https://doi.org/10.59400/sv4216

ARTICLE INFO

Received: 1 March 2026
Revised: 21 April 2026
Accepted: 27 April 2026
Available online: 23 June 2026

Abstract: To address the issues of low fitting accuracy, parameter selection relying on empirical judgment, and difficulties in quantifying model robustness in the traditional Sadovsky blasting vibration prediction formula, this study proposes a method for modifying the peak particle velocity prediction model that balances fitting capability and robustness by integrating Bayesian theory with dimensional analysis. A model prior distribution incorporating multiple on-site blasting parameters is constructed using the dimensional π theorem. Within the Bayesian framework, the maximum likelihood estimation, Occam factor, and posterior credibility of the model are calculated to achieve automatic selection of influencing factors and optimization of the model structure. Based on 88 sets of measured data from an open-pit quarry, with 70 sets used as training samples and 18 sets as validation samples, model training and validation are conducted. The results show that the coefficient of determination R^2 of the Bayesian modified model increases from 0.7749 obtained by the traditional Sadovsky formula to 0.8576. The Occam factor can effectively characterize the robustness of the model. The preferred model "1 2 4" incorporates empirical formulas for correcting the resistance line, spacing between rows, and borehole diameter. This model achieves an optimal balance between prediction accuracy and robustness, and its prediction stability is significantly superior to that of traditional empirical formulas. This method provides a theoretical basis and engineering reference for accurate prediction and safety control of blasting vibrations.

Keywords: blasting vibration; peak particle velocity (PPV); prediction model optimization; dimensional analysis; Bayesian theory; model robustness; open-pit mine blasting

1. Introduction

Due to the rapid development of mining, water conservancy and hydropower projects, and transportation infrastructure construction, blasting, as an efficient and low-cost construction method, has been widely applied in various large-scale projects [1,2]. However, during the blasting process, a portion of the explosive energy dissipates while fracturing the target rock mass, simultaneously inducing adverse effects such as ground vibration, air overpressure, and flyrock, which may cause damage to surrounding structures, casualties, and economic losses. Among these, vibration is considered the primary adverse effect of blasting due to its significant impact on the surrounding environment [3, 4]. Therefore, predicting and controlling

blasting-induced vibration holds considerable practical significance.

In the mid-20th century, researchers worldwide, based on extensive field test data, developed empirical formulas for predicting blasting vibration that were tailored to local conditions [5]. Although the empirical formulas vary across different countries and regions, they have been widely adopted in the field of blasting vibration prediction due to their ability to provide fast and accurate estimates of peak particle velocity [6].

As research progressed, scholars recognized that empirical formulas could not meet the demands of all engineering conditions and began exploring alternative methods for predicting blasting vibration. Current research on blasting vibration prediction primarily focuses on three approaches: numerical simulation, computer algorithm–based fitting, and empirical formula modification.

Numerical simulation methods [7,8], based on software platforms such as ANSYS, rely on the mechanical parameters of the rock mass and explosives obtained from field tests to establish numerical models that simulate the physical process of blasting, thereby enabling the prediction of peak particle velocity. Gou et al. [9], addressing the limitations of traditional prediction methods, introduced response spectrum analysis and normalized pseudo-velocity response spectra to develop a novel method for characterizing ground motion. Wang et al. [10] established an IA-BP inverse analysis method and validated the inverted parameters of the JH-2 constitutive model through numerical simulation, obtaining linear attenuation formulas for peak particle velocity at the tunnel crown, arch shoulder, and arch foot, thereby providing reliable predictions for subsequent construction safety. Zhang et al. [11] analyzed the transformation relationship between blasting vibration input energy and the elastic strain energy and kinetic energy of concrete mass elements, and derived a safe peak particle velocity control value for an existing tunnel by combining numerical simulation with the energy criterion for concrete damage. However, the process of establishing numerical models is time-consuming and labor-intensive, and the results are often difficult to apply directly in engineering blasting design.

Computer algorithm–based fitting methods [12–14] utilize algorithms such as genetic algorithms and artificial neural networks to construct predictive models based on measured data, achieving high fitting accuracy. Fissha et al. [15] employed relevance vector machine methods, using peak particle velocity as the key evaluation indicator, and applied both conventional and optimized RVM models to ground vibration prediction. Aruna et al. [16] developed an IoT-based ground vibration monitoring device combined with machine learning algorithms to achieve intelligent prediction of vibration intensity. Hosseini et al. [17] constructed two ensemble models—an artificial neural network ensemble and an extreme gradient boosting ensemble—and integrated them using stacking generalization techniques to obtain final prediction results. However, such methods often disregard the interrelationships and variation patterns among physical quantities, lack explicit physical significance, and are prone to overfitting, thereby exhibiting certain limitations in practical engineering applications.

Empirical formula modification methods [18–20] introduce site-specific parameters such as elevation, borehole diameter, and borehole spacing based on the unique conditions of field blasting, and establish new prediction formulas using

dimensional analysis on the basis of the traditional Sadovsky empirical formula. Wang et al. [21] developed a prediction formula for blasting vibration duration using frequency and energy as independent variables and analyzed it using the statistical t-distribution, obtaining the delay time required for a structure to reach its resonance frequency by calculating its dominant frequency. Khan et al. [22] applied the United States Bureau of Mines formula to analyze the correlation between scaled distance and particle velocity, and established a peak particle velocity prediction equation applicable to the study area through statistical regression. Guan et al. [23] analyzed the cavity amplification effect of an excavated tunnel and its influence on the propagation of blasting seismic waves, introducing an amplification coefficient to modify the traditional prediction formula and establishing an improved model for predicting near-field PPV using far-field monitoring data. Nevertheless, the selection of influencing factors in most studies relies heavily on expert experience, and a rapid and reliable method for factor selection has yet to be developed. The manual selection approach often fails to identify all relevant influencing factors, thereby limiting the fitting accuracy of the modified formulas.

In the 1990s, Beck [24] first proposed the concept of model updating based on Bayesian theory. This method addresses inherent uncertainties within the framework of Bayesian statistics, providing a rational and computationally feasible approach to predicting structural responses. As an effective means of handling modeling uncertainties, Bayesian theory has been extensively developed in various fields such as finance, aerospace, and civil engineering.

This paper introduces Bayesian theory into the field of blasting vibration prediction. By combining dimensional analysis, a method for updating blasting vibration prediction models is proposed from both physical and statistical perspectives, aiming to balance data fitting accuracy and robustness, and to address the issue of selecting site-specific influencing factors. The accuracy of the proposed method is validated through field case studies.

2. Bayesian theory

Bayesian theory and classical probability theory both belong to the domain of mathematical statistics. However, Bayesian theory treats parameters as random variables, embodying an analytical approach that better represents uncertainty. Bayesian theory is developed based on the law of total probability:

$$P(A|B) = \frac{P(B|A)P(A)}{P(B)}, \tag{1}$$

Where A and B denote two independent events. $P(A)$ represents the prior probability. Before observing the new evidence B, it is the initial judgment of the probability of event A occurring. $P(B)$ represents the probability of evidence. It is the total probability of observing evidence B in all possible scenarios, and it serves the role of normalization. $P(B|A)$ represents the likelihood function. Assuming that event A is true, it represents the probability of observing evidence B. $P(A|B)$ represents the posterior probability. After observing evidence B, the updated probability of event A

occurring is this value, which is the result of Bayesian inference.

Suppose parameter D represents a set of monitoring data consisting of N discrete points, parameter C represents the set of all possible model forms that may exist, and parameter μ represents the initial judgment of the model prior to computation. Based on the above parameters and using the total probability formula, the probabilities of each model C_j under the known conditions D, μ can be obtained:

$$P(C_j|D,\mu) = \frac{P(D|C_j,\mu)P(C_j|\mu)}{P(D|\mu)}, \tag{2}$$

Where $P(D|\mu)$ can be decomposed using the law of total probability as:

$$P(D|\mu) = \sum\nolimits_{j=1}^{N_c} P(D|C_j,\mu)P(C_j|\mu). \tag{3}$$

In the formula, $P(C_j|\mu)$ represents the occurrence probability of the jth model C_j when the parameter μ is known. $P(D|C_j,\mu)$ represents the probability of parameter D occurring when the jth model C_j and parameter μ are known; N_c indicates the number of parameters C.

To facilitate computation, the prior distribution $P(C_j|\mu)$ is normalized:

$$\sum\nolimits_{j=1}^{N_c} P(C_j|\mu) = 1. \tag{4}$$

The initial judgment μ of the model has no direct relationship with $P(D|C_j,\mu)$, so it can be disregarded. After simplification, the Laplace expansion of $P(D|C_j)$ is approximately.

Use $\theta_j \in R^{N_j}$ to denote the uncertain parameter vector in the parameter space Θ_j for model class C_j, where N_j is the number of uncertain parameters. By the theorem of total probability, the evidence of C_j is given by:

$$P(D|C_j) = \int_{\Theta_j} P(D|\theta_j,C_j)P(\theta_j|C_j)d\theta_j, \tag{5}$$

where $P(D|\theta_j,C_j)$ is the likelihood function of model class C_j and $P(\theta_j|C_j)$ is the prior distribution of the uncertain parameters. For a large number of data points, the integrand in the evidence integral in Equation (5) can be well approximated as an unnormalized Gaussian distribution, so this evidence integral can be approximated by Laplace's asymptotic approximation:

$$P(D|C_j) \approx P(D|\theta^*,C_j)O_j. \tag{6}$$

θ^* is the optimal parameter vector that maximizes the integrand in Equation (5) and the Ockham factor O_j represents the penalty against complicated parameterization:

$$O_j = P(\theta^*|C_j)(2\pi)^{\frac{N_j}{2}} |_j(\theta^*)|^{-\frac{1}{2}}. \tag{7}$$

The matrix $_j(\theta^*)$ is the Hessian matrix of objective function $-ln[P(D|\theta_j,C_j)P(\theta_j|C_j)]$ evaluated at $\theta_j = \theta_j^*$. By Equation (6), the evidence of a model class represents

the competition between data fitting capability (measured by the maximum likelihood value $P(D|\theta^*, C_j)$ and the robustness of the model class (measured by the Ockham factor)) [25].

To enhance the model's fitting capability, a common approach is to incorporate additional relevant parameters. However, increasing the number of parameters also reduces the model's robustness. Low robustness increases model sensitivity, thereby amplifying the impact of model uncertainty on prediction results, and may even render the model inapplicable due to excessive errors [26]. Therefore, it is necessary to achieve a balance between these two attributes.

The modification of a blasting vibration prediction model can be regarded as a linear solution process, generally expressed by Equation (8):

$$D(x;\theta,C_j)=\sum\nolimits_{l=1}^{N_b}\theta_l x_l+\varepsilon. \tag{8}$$

In the formula, ε follows a Gaussian distribution with a mean of zero and a variance of σ_ε^2, representing the model parameters and the uncertainty in modeling, which includes measurement noise and modeling errors. x_l represents the parameters of the prediction model, which are determined by the adopted blasting vibration prediction model; θ_l is the scaling parameter, used to correct the blasting vibration model; N_θ is the number of model parameters.

The likelihood function measures the probability of generating the current set of data under model C_j. The higher the probability, the better the model fits. Assuming that the prediction errors for each record are statistically independent, the likelihood function is obtained as follows:

$$P(D|\theta,C_j)=(2\pi\sigma_\varepsilon^2)^{-\frac{N}{2}}e^{-\frac{N}{2\sigma_\varepsilon^2}J_g(\theta|D,C_j)}. \tag{9}$$

In the formula, $J_g(\theta|D,C_j)$ is referred to as the goodness-of-fit function, which indicates the degree of data fitting.

$$J_g(\theta|D,C_j)=\frac{1}{N}\sum\nolimits_{n=1}^{N}\left[y(n)-\sum\nolimits_{l=1}^{N_b}\theta_l x_l\right]^2. \tag{10}$$

In the formula, $y(n)$ represents the measured peak vibration velocity of the blasting, and N represents the number of blasting vibration data.

To solve the equation, it is necessary to determine the probability density function of the prior distribution of the model, that is, to obtain the optimal vector θ^* by minimizing $J_g(\theta|D,C_j)$:

$$\theta^*=A^{-1}\begin{bmatrix}\frac{1}{N}\sum_{n=1}^{N}x_1(n)y(n)\\ \frac{1}{N}\sum_{n=1}^{N}x_2(n)y(n)\\ \vdots\\ \frac{1}{N}\sum_{n=1}^{N}x_\theta(n)y(n)\end{bmatrix}. \tag{11}$$

In the formula, A represents a symmetric matrix of $N_\theta \times N_\theta$:

$$A = \frac{1}{N}\sum\nolimits_{n=1}^{N} x(n)x(n)^T. \tag{12}$$

Minimizing the goodness-of-fit function is essentially equivalent to obtaining the variance of the model prediction:

$$\sigma_\varepsilon^{2^*} = min_b J_g(\theta|D, C_j) = min_b J_g(\theta^*|D, C_j). \tag{13}$$

Following the above assumptions, the maximum likelihood function and the Occam factor of the model can be expressed as shown in Equations (14) and (15).

$$P(D|\theta^*, C_j) = P(D|\theta, C_j) = (2\pi\sigma_\varepsilon^2)^{-\frac{N}{2}} e^{-\frac{N}{2}}, \tag{14}$$

$$O_j = P(\theta^*|C_j)(2\pi)^{\frac{N_j}{2}} |_j(\theta^*)|^{-\frac{1}{2}} = P(\theta^*|C_j)|A|^{-\frac{1}{2}}(\frac{\pi}{N})^{\frac{N_j}{2}}(\sqrt{2}\sigma_\varepsilon^*)^{N_j+1}. \tag{15}$$

In the formula, N_j represents the number of unknown parameters in Model C_j that are subject to uncertainty.

3. Prediction of blasting peak particle velocity based on Bayesian theory

3.1. Engineering background

In order to accurately verify and present the significant advantages of the Bayesian theory-corrected prediction model in the prediction of blasting vibrations in complex rock masses, this paper selects an open-pit quarry with typical layered sedimentary rock structural characteristics as the engineering background. The geological conditions of this quarry are relatively complex. The excavated rock mass mainly consists of interbedded sandstone and shale, crushed sandstone fracture zones, and weak mudstone interlayers with heterogeneous rock properties. The rock mass is characterized by the development of joint and fracture fissures, with prominent anisotropic features, which significantly affect the propagation and attenuation laws of blasting seismic waves. Therefore, it can fully test the applicability and accuracy of the corrected prediction model in actual working conditions.

During the blasting construction process, this project fully adopted high-precision digital electronic detonators for sequential hole detonation, achieving millisecond-level precise delay control. This effectively reduced the amount of explosives per segment and optimized the superimposition effect of blasting vibrations. According to the height of the bench, the explosibility of the rock mass, and the production schedule requirements, each blasting operation typically sets 2 to 4 rows of main blast holes. The number of blast holes in each row is adjusted dynamically based on the free surface conditions on the site, the distribution of resistance lines, and the terrain undulation, ranging from 10 to 30. To ensure uniform blasting block size and control the rebound and base, the main blast holes are arranged in a staggered pattern. The maximum charge amount per hole is restricted by the hole depth, hole diameter, and rock properties, with a variation range of 55 kg to 227 kg. The charge structure inside the hole adopts

continuous or spaced coupling charging methods, and an appropriate blocking length is added to maintain the efficiency of explosive energy utilization.

While conducting real-time monitoring of blasting vibration velocities, systematic collection and organization of the on-site blasting design parameters were carried out. Based on the above monitoring and collection work, 88 sets of reliable blasting vibration events with high data quality were selected from the blasting database as the total sample. Each sample included the corresponding three-dimensional peak vibration velocity, main frequency, vibration duration, as well as propagation path parameters such as the horizontal distance from the blast source center and elevation difference.

To construct and validate the Bayesian theory-corrected prediction model, this study built a prediction correction model based on the Bayesian statistical inference framework. Following the general paradigm for validating machine learning models, all 88 sets of data were randomly divided into a training set (n = 70) and a validation set (n = 18) in a ratio of approximately 8:2. The random partitioning process ensured the consistency of the distribution characteristics of the two sets. The training set was used for the prior setting and posterior inference of the model parameters, while the validation set independently evaluated the generalization performance of the model. The model did not introduce additional hyperparameters, and the training process was terminated based on the convergence of the likelihood function and the stabilization of the coefficient of determination R^2.

3.2. Construction of the prior model based on dimensional analysis

To ensure the physical significance of the peak particle velocity prediction model, dimensional analysis was employed to derive the prior distribution of the model. A total of 10 on-site blasting parameters were recorded: maximum charge weight per hole, blast center distance, burden length, row spacing, bench height, stemming length, borehole subdrilling, borehole diameter, vibration wave velocity, and rock mass density. If conventional dimensional analysis were applied, the large number of dependent variables would result in a lengthy formula, and the establishment of the posterior distribution of the model would lead to dimensional inconsistency between the two sides of the equation. Therefore, parameters such as burden length, row spacing, bench height, stemming length, borehole subdrilling, and borehole diameter were processed to eliminate their units, allowing them to participate in the model establishment process only as dimensionless parameters, as detailed in **Table 1**.

Table 1. Parameters required for prior distribution of the model.

Parameter	Symbol	Unit	Dimension
Maximum charge per hole	Q	kg	M
Blast center distance	R	m	L
Row spacing/Burden length	S/B	\	\
Bench height/Burden length	H/B	\	\
Burden length/Borehole diameter	B/D	\	\
Stemming length/Burden length	T/B	\	\
Borehole subdrilling/Burden length	U/B	\	\
Vibration wave velocity	c	m/s	LT^{-1}
Rock mass density	ρ	kg/m^3	ML^{-3}
Peak particle velocity	v	m/s	LT^{-1}

According to the dimensional analysis π theorem, taking c, R, Q as independent dimensions, using the 10 mutually independent parameters in **Table 1**, 7 functions about π_i are formed:

$$\begin{cases} \pi = \frac{v}{c} & \pi_1 = \frac{\rho}{QR^{-3}} & \pi_2 = \frac{S}{B} \\ \pi_3 = \frac{H}{B} & \pi_4 = \frac{B}{D} & \pi_5 = \frac{T}{B} \quad \pi_6 = \frac{U}{B} \end{cases}. \tag{16}$$

Therefore, the peak particle velocity function relationship of the particle can be expressed by Equation (17). Under normal circumstances, it is assumed that the propagation speed of the seismic wave and the density of the rock mass are constants within the blasting area. After multiplying the parameters on both sides of Equation (17) and then taking the exponent with base e simultaneously, Equation (18) can be obtained.

$$\frac{v}{c} = f(\frac{\rho}{QR^{-3}}, \frac{S}{B}, \frac{H}{B}, \frac{B}{D}, \frac{T}{B}, \frac{U}{B}), \tag{17}$$

$$ln(v) = a + b_1 ln(\frac{\sqrt[3]{Q}}{R}) + b_2 ln(\frac{S}{B}) + b_3 ln(\frac{H}{B}) + b_4 ln(\frac{B}{D}) + b_5 ln(\frac{T}{B}) + b_6 ln(\frac{U}{B}). \tag{18}$$

3.3. Bayesian theory for predicting blast velocity steps

The relationship between the complexity of the model, output sensitivity, data capacity, and robustness directly determines the quality of the output results. Influenced by forward modeling thinking, researchers tend to adopt complex model types to cover more physical behaviors. However, the more complex the model is, the more uncertain parameters there usually are. Due to the accumulation of small errors in multiple parameters, the output error will increase, and even lead to the problem of model unidentifiability. Therefore, a model with an appropriate complexity should be selected.

Equation (18) includes almost all the on-site blasting parameters that can be obtained. However, the complex calculation formula is neither applicable for practical use nor can it avoid the accumulation of small errors from multiple parameters, which would lead to an increase in output errors. To select a model with an appropriate complexity from among these, Equation (18) needs to be processed:

Step 1: The model's prior distribution is sequentially divided into six types of variables according to the order of coefficient θ. Among them, variable 1 corresponds to the traditional Sadovsky formula, that is, $a + b_1 ln(\sqrt[3]{Q}/R)$, which is a mandatory basic term; Variable 2 represents the ratio of the pitch distance to the resistance line, which is denoted as $ln(S/B)$; Variable 3 represents the ratio of the step height to the resistance line, which is denoted as $ln(H/B)$; Variable 4 represents the ratio of the resistance line to the borehole diameter, which is denoted as $ln(B/D)$; variable 5 represents the ratio of the plug length to the resistance line, denoted as $ln(T/B)$; variable 6 represents the ratio of the over-depth of the borehole to the resistance line, denoted as $ln(U/B)$.

Step 2: After fixing the necessary variables of the vibration model, the remaining 5 variables are fully combined based on whether they are involved or not. This results in a total of $2^5 = 32$ different model structures, achieving an orderly traversal from the basic formula to the multi-parameter expansion.

Step 3: For each model configuration, the parameters in the Bayesian formula are

assigned accordingly, and the corresponding variance, maximum likelihood estimate, Occam factor, and credibility are calculated.

4. Analysis of Bayesian theory prediction results

4.1. Result and analysis

The calculation results are shown in **Table 2**. The 32 models are ranked in order of reliability. The model "**1 2 3 4 5 6**" represents the prior distribution of the model. Its fitting coefficient R^2 = 0.858, and the maximum likelihood estimate $lnP(D|\theta^*, C_7) = 6.28 \times 10^{-3}$ is the maximum value among all models. However, its robustness is inferior to that of other models, and its Occam factor is only $lnO_7 = 4.31 \times 10^{-5}$, which is the smallest among all models. Model "**1**" represents Sadovsky's empirical formula. Its Occam factor is the maximum at $lnO_1 = 1.32 \times 10^{-5}$, but its corresponding fitting coefficient R^2 = 0.775, and $lnP(D|\theta^*, C_j) = 1.14 \times 10^{-11}$ is smaller than that of other models. This phenomenon is in line with the actual situation, that is, the more parameters introduced in the prediction model, the lower its robustness, while its prediction accuracy is higher.

Table 2. Processing results of Bayesian method.

Sequence	Model parameter combination	σ_ε^{2*}	$lnP(D\|\theta^*, C_j)$	lnO_i	$P(C_j\|D, \mu)$	a	b_1	b_2	b_3	b_4	b_5	b_6	R^2
1	1 2 4 6	0.066	−5.36	−9.30	1.71×10^{-1}	0.49	1.83	1.08		2.11		0.34	0.8566
2	1 2 4	0.067	−6.11	−8.83	1.29×10^{-1}	−0.05	1.84	0.99		2.13			0.8541
3	1 2 4 5 6	0.066	−5.28	−9.84	1.08×10^{-1}	0.32	1.84	1.04		2.16	0.10	0.34	0.8569
4	1 2 3 4 5	0.067	−5.77	−9.99	9.25×10^{-2}	0.00	1.86	0.99	−0.16	2.18	0.21		0.8553
5	1 2 3 4 6	0.066	−5.29	−10.05	8.69×10^{-2}	0.68	1.84	1.13	−0.08	2.08		0.34	0.8569
6	1 2 4 5	0.067	−6.00	−9.36	8.48×10^{-2}	−0.24	1.85	0.94		2.19	0.12		0.8545
7	1 2 3 4 5 6	0.066	−5.07	−10.43	7.40×10^{-2}	0.54	1.85	1.09	−0.15	2.15	0.19	0.33	0.8576
8	1 2 3 4	0.067	−6.04	−9.58	6.56×10^{-2}	0.13	1.84	1.03	−0.08	2.10			0.8544
9	1 4 6	0.068	−6.60	−9.58	3.71×10^{-2}	1.56	1.84			1.82		0.29	0.8525
10	1 4	0.069	−7.15	−8.05	3.69×10^{-2}	1.01	1.85			1.86			0.8507
11	1 4 5 6	0.068	−6.40	−10.19	2.48×10^{-2}	1.22	1.85			1.92	0.16	0.29	0.8532
12	1 4 5	0.069	−6.92	−9.68	2.48×10^{-2}	0.66	1.86			1.97	0.17		0.8515
13	1 3 4 6	0.068	−6.60	−10.40	1.65×10^{-2}	1.63	1.85		−0.02	1.81		0.29	0.8525
14	1 3 4	0.069	−7.14	−9.91	1.57×10^{-2}	1.08	1.85		−0.03	1.85			0.8507
15	1 3 4 5 6	0.068	−6.28	−10.79	1.54×10^{-2}	1.42	1.86		−0.11	1.91	0.23	0.28	0.8536
16	1 3 4 5	0.068	−6.78	−10.29	1.54×10^{-2}	0.88	1.87		−0.12	1.95	0.24		0.8519
17	1 2 5 6	0.094	−20.86	−7.63	1.69×10^{-7}	7.61	1.74	−0.85			−0.45	0.45	0.7961
18	1 2 5	0.096	−21.79	−6.77	1.58×10^{-7}	6.98	1.75	−1.02			−0.44		0.7917
19	1 2 3 5 6	0.093	−20.50	−8.17	1.41×10^{-7}	7.88	1.76	−0.76	−0.23		−0.31	0.45	0.7977
20	1 2 3 6	0.094	−20.98	−7.87	1.18×10^{-7}	8.05	1.77	−0.94	−0.37			0.43	0.7955
21	1 2 3 5	0.095	−21.41	−7.56	1.05×10^{-7}	7.27	1.76	−0.92	−0.24		−0.29		0.7935
22	1 2 3	0.096	−21.81	−7.21	9.86×10^{-8}	8.06	1.75	−0.47	0.50				0.7916
23	1 2	0.099	−23.00	−6.35	7.16×10^{-8}	7.03	1.76	−1.46					0.7859
24	1 2 6	0.097	−22.18	−7.19	7.05×10^{-8}	7.63	1.75	−1.31				0.43	0.7899
25	1 5 6	0.095	−21.51	−8.20	4.98×10^{-8}	7.51	1.71				−0.57	0.52	0.7930
26	1 3 5 6	0.094	−21.02	−8.75	4.67×10^{-8}	7.84	1.74		−0.27		−0.40	0.50	0.7953
27	1 5	0.098	−22.74	−7.15	4.17×10^{-8}	6.75	1.72				−0.58		0.7872
28	1 3 6	0.096	−21.82	−8.42	2.93×10^{-8}	8.06	1.75		−0.47			0.50	0.7916
29	1 3 5	0.097	−22.18	−8.10	2.82×10^{-8}	7.13	1.74		−0.30		−0.39		0.7899
30	1 3	0.099	−22.95	−7.74	1.88×10^{-8}	7.35	1.76		−0.49				0.7862
31	1 6	0.101	−23.94	−7.64	7.64×10^{-9}	7.47	1.71					0.54	0.7813
32	1	0.104	−25.20	−6.63	6.00×10^{-9}	6.67	1.72						0.7749

The model composed of variable 1 and the other 5 variables is shown in **Table 3**. Among them, model "**1 4**", $ln(v) = a + b_1 ln(\sqrt[3]{Q}/R) + b_4 ln(B/D)$, has a higher fitting coefficient than the other models, indicating that the diameter of the blast holes has a significant impact on the blasting vibration of this open-pit mine. From this, it can be seen that the influence of the variables on the blasting vibration, from greatest to least, is B/D, T/B, H/B, S/B and U/B. **Table 4** presents the model arrangement in descending order based on the fitting coefficient R^2. The maximum likelihood

estimation in the table decreases as the fitting coefficient decreases. Therefore, the maximum likelihood estimation of the model can represent the model fitting coefficient when evaluating the fitting ability of the model.

Table 3. Arrangement of different two-parameter combination models.

Sequence	Model parameter combination	Model form	$lnP(D\|\theta^*, C_j)$	R^2
1	1 4	$ln(v)=a+b_1ln(\frac{\sqrt[3]{Q}}{R})+b_4ln(\frac{B}{D})$	−7.15	0.8507
2	1 5	$ln(v)=a+b_1ln(\frac{\sqrt[3]{Q}}{R})+b_5ln(\frac{T}{B})$	−22.74	0.7872
3	1 3	$ln(v)=a+b_1ln(\frac{\sqrt[3]{Q}}{R})+b_3ln(\frac{H}{B})$	−22.95	0.7862
4	1 2	$ln(v)=a+b_1ln(\frac{\sqrt[3]{Q}}{R})+b_2ln(\frac{S}{B})$	−23	0.7859
5	1 6	$ln(v)=a+b_1ln(\frac{\sqrt[3]{Q}}{R})+b_6ln(\frac{U}{B})$	−23.94	0.7813

Table 4. The fitting degree is the descending order of model arrangement.

Sequence	Model parameter combination	$lnP(D\|\theta^*, C_j)$	R^2	Sequence	Model parameter combination	$lnP(D\|\theta^*, C_j)$	R^2
1	1 2 3 4 5 6	−5.07	0.8576	17	1 2 3 5 6	−20.5	0.7977
2	1 2 4 5 6	−5.28	0.8569	18	1 2 5 6	−20.86	0.7961
3	1 2 3 4 6	−5.29	0.8569	19	1 2 3 6	−20.98	0.7955
4	1 2 4 6	−5.36	0.8566	20	1 3 5 6	−21.02	0.7953
5	1 2 3 4 5	−5.77	0.8553	21	1 2 3 5	−21.41	0.7935
6	1 2 4 5	−6	0.8545	22	1 5 6	−21.51	0.793
7	1 2 3 4	−6.04	0.8544	23	1 2 5	−21.79	0.7917
8	1 2 4	−6.11	0.8541	24	1 2 3	−21.81	0.7916
9	1 3 4 5 6	−6.28	0.8536	25	1 3 6	−21.82	0.7916
10	1 4 5 6	−6.4	0.8532	26	1 2 6	−22.18	0.7899
11	1 4 6	−6.6	0.8525	27	1 3 5	−22.18	0.7899
12	1 3 4 6	−6.6	0.8525	28	1 5	−22.74	0.7872
13	1 3 4 5	−6.78	0.8519	29	1 3	−22.95	0.7862
14	1 4 5	−6.92	0.8515	30	1 2	−23	0.7859
15	1 4	−7.15	0.8507	31	1 6	−23.94	0.7813
16	1 3 4	−7.14	0.8507	32	1	−25.2	0.7749

In **Table 2**, the credibility of model "**1 2 4 6**", $ln(v) = a + b_1ln(\sqrt[3]{Q}/R) + b_2ln(S/B) + b_4ln(B/D) + b_6ln(U/B)$, is the highest at 17.1%, while model "**1 2 4**", $ln(v) = a + b_1ln(\sqrt[3]{Q}/R) + b_2ln(S/B) + b_4ln(B/D)$, has a credibility of 12.9%, ranking second only to model "**1 2 4 6**". Although both models' Occam factor and fitting coefficient are not the optimal choices, considering the comprehensive factors of model's anti-interference and fitting ability, these two vibration speed prediction models are ranked at the top. The credibility and fitting coefficient of the two models differ by 4.2% and 0.025 respectively, and the difference is relatively small. Therefore, both models meet the requirements. However, compared to model "**1 2 4 6**", model "**1 2 4**" has fewer parameters, which not only makes it more robust but also more convenient to operate during actual measurement. In conclusion, model "**1 2 4**" is the optimal blasting vibration prediction model, as shown in Equation (19):

$$v = 0.95(\frac{\sqrt[3]{Q}}{R})^{1.84}(\frac{S}{B})^{0.99}(\frac{B}{D})^{2.13} \tag{19}$$

4.2. Comparison of prediction results between Bayesian theory and the Sadovsky formula

The 18 randomly selected verification sample data were respectively input into the Sadovsky empirical formula, $ln(v) = a + b_1 ln(\sqrt[3]{Q}/R)$, and Model "**1 2 4**", $ln(v) = a + b_1 ln(\sqrt[3]{Q}/R) + b_2 ln(S/B) + b_4 ln(B/D)$, and Model "**1 2 4 6**", $ln(v) = a + b_1 ln(\sqrt[3]{Q}/R) + b_2 ln(S/B) + b_4 ln(B/D) + b_6 ln(U/B)$. Three comparison charts of predicted versus actual vibration were plotted, as shown in **Figure 1**. As illustrated in **Figure 1a**, the prediction error of the Sadovsky empirical formula increases with vibration magnitude. When the vibration is within 10 mm/s, its prediction remains relatively accurate. **Figure 1b,c** show that the prediction results of Model "**1 2 4**" and Model "**1 2 4 6**" are essentially consistent, with prediction errors remaining stable and exhibiting no significant variation as vibration magnitude increases. Therefore, in the field of predicting blasting vibration, the models "**1 2 4**" and "**1 2 4 6**" based on Bayesian theory are superior to the Sadovsky empirical formula.

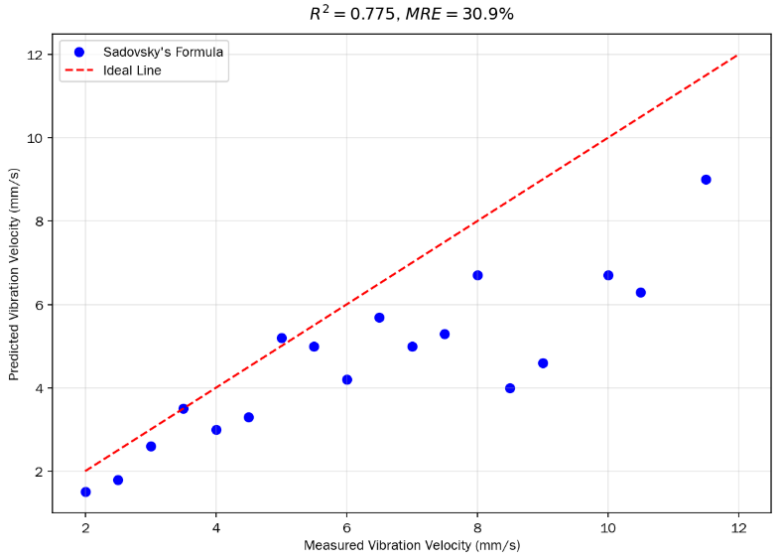

(a) Comparison chart of predictions by the Sadovsky formula versus peak particle velocity.

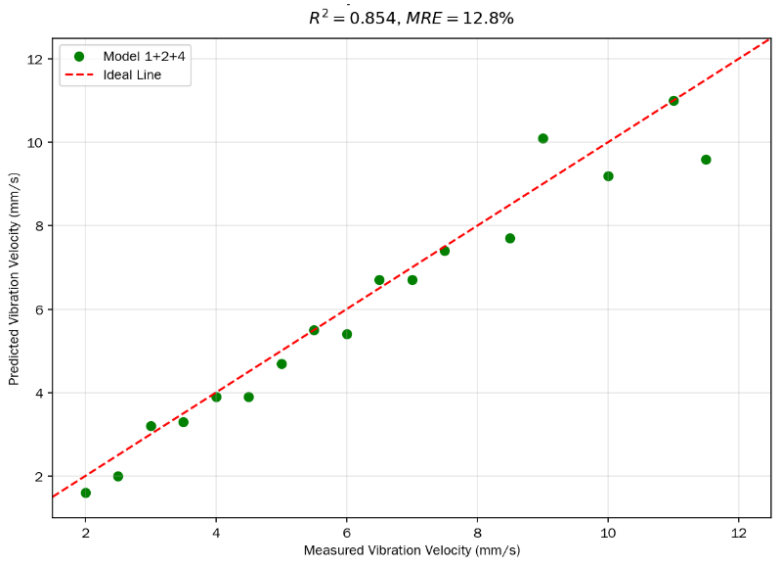

(b) Comparison chart of predictions by Model "**1 2 4**" versus peak particle velocity.

Figure 1. *Cont.*

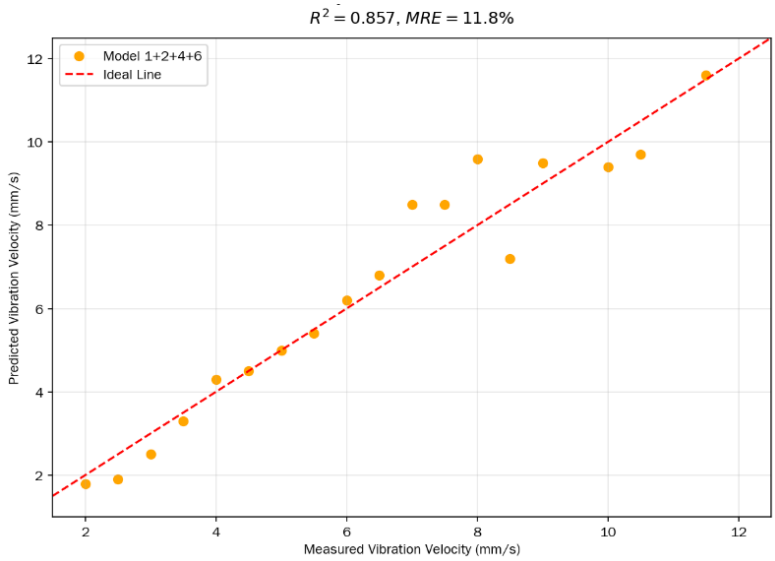

(c) Comparison chart of predictions by Model "**1 2 4 6**" versus peak particle velocity.

Figure 1. Comparison of predicted and measured vibration velocities.

To verify the robustness of the three models under the interference of actual measurement errors, this study designed the following sensitivity test scheme based on the error propagation characteristics of the measurement system: In all input parameters of the 18 verification samples, ±10% random errors following a uniform distribution were superimposed. It should be noted that a unified ±10% perturbation amplitude was selected here, not because the differences in measurement accuracy of different parameters were ignored, but based on the principle of most unfavorable conservatism: in the engineering site, the relative measurement errors of main physical parameters such as charge quantity, explosion center distance, and bore diameter are usually controlled within ±5%. Considering the superposition of measurement errors and environmental influences in extreme conditions, it is extended to ±10%, which can cover the vast majority of non-ideal test scenarios. Therefore, if the models still perform stably under this wide range of perturbations, it can be considered that they have sufficient anti-interference margin in practical applications.

The perturbed parameters are re-input into the model for vibration velocity prediction, and the corresponding three model prediction results are plotted based on **Figure 1**. The robustness of the model is characterized by comparing the deviations before and after perturbation, as shown in **Figure 2**. In **Figure 2**, the prediction accuracy of the three models all increases with the increase in vibration velocity; when the vibration velocity is below 10 mm/s, the Sadovskiy empirical formula and model "**1 2 4**" show strong anti-interference ability, while as the vibration velocity further increases, the deviation between the two and the benchmark prediction value in **Figure 1** gradually becomes larger; model "**1 2 4 6**" shows higher disturbance sensitivity in all vibration velocity ranges. In summary, compared to model "**1 2 4 6**", model "**1 2 4**" shows stronger robustness under unified strict interference conditions and can better adapt to the uncertainty of on-site measurement. From a theoretical perspective, model "**1 2 4 6**" has more parameters introduced and a higher model complexity, resulting in a smaller Occam factor and weaker robustness, which conforms to the Bayesian model

rule of "increased complexity→decreased robustness".

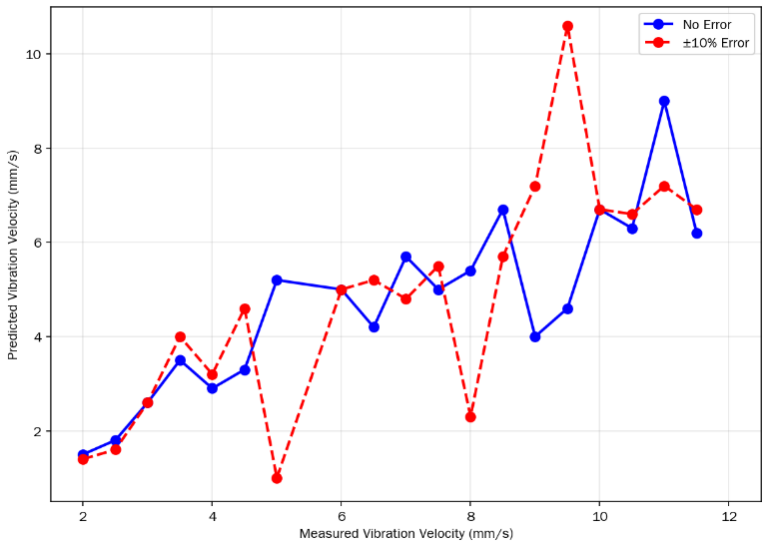

(a) Comparison chart of predictions by the Sadovsky formula versus peak particle velocity with a 10% error margin.

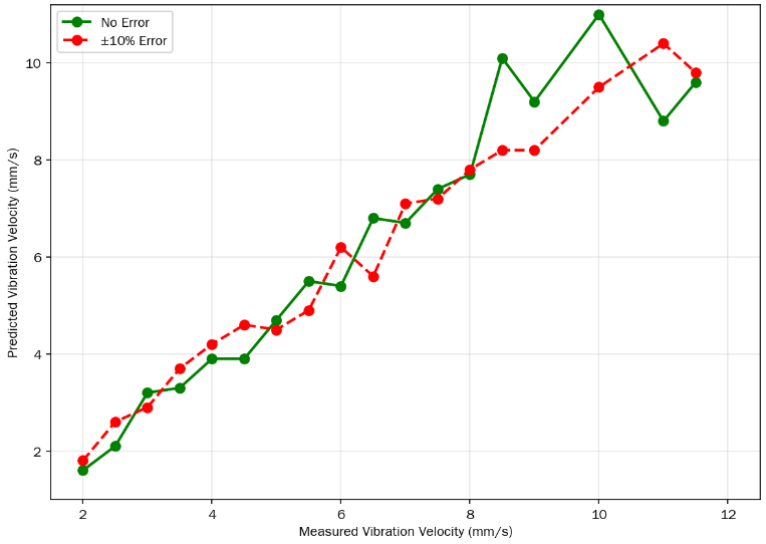

(b) Comparison chart of predictions by Model "**1 2 4**" versus peak particle velocity with a 10% error margin.

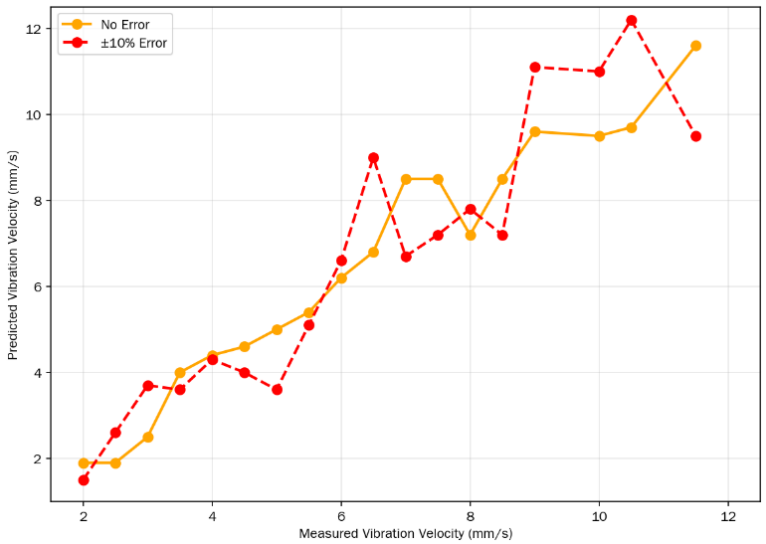

(c) Comparison chart of predictions by Model "**1 2 4 6**" versus peak particle velocity with a 10% error margin.

Figure 2. Comparison of robustness of the three models.

5. Conclusion

To address the limitations of existing blasting vibration prediction models, this paper introduces Bayesian theory combined with dimensional analysis and proposes a method for correcting blasting vibration prediction models that accounts for parameter uncertainty and is supported by mathematical theory. The main conclusions are as follows:

The correction of a prediction model requires a balance between fitting capability and robustness. From the perspective of probability and statistics, Bayesian theory defines the Occam factor to represent model robustness. It is verified through case studies that a larger Occam factor corresponds to higher model robustness. This factor effectively characterizes the model's anti-interference ability, achieving a balance between goodness of fit and robustness, thereby avoiding overfitting.

The prior distribution of the model is derived using dimensional analysis combined with on-site blasting parameters. Based on this prior distribution, Bayesian theory determines the optimal blasting vibration prediction model by calculating the model credibility. When the credibility values differ only slightly, it is necessary to consider both site conditions and credibility to select the optimal model.

Compared with the traditional Sadovsky empirical formula, the prediction model corrected by Bayesian theory not only balances data fitting and anti-interference capability but also automatically selects the primary influencing factors from numerous parameters, thereby achieving stronger fitting performance. This theory enables the automatic identification of key influencing factors based on multiple on-site parameters, replacing the traditional parameter selection approach that relies on empirical judgment, and significantly enhances the scientific rigor and generalizability of the model.

This model is established based on the blasting of open-pit steps of sandstone-shale type, and is applicable to similar rock types and blasting conditions of open-pit steps; it is not applicable to chamber blasting, underground deep-hole blasting, and extremely fractured and weak rock masses. When it is promoted, it is necessary to retrain and calibrate based on the geological conditions of the site area.

Author contributions: Conceptualization, BJ; methodology, BJ; software, BJ; validation, XW; formal analysis, BJ; investigation, ZL; resources, ZX; data curation, LQ; writing—original draft preparation, BJ; writing—review and editing, BJ; visualization, XW; supervision, BJ; project administration, BJ; funding acquisition, BJ. All authors have read and agreed to the published version of the manuscript.

Funding: This work was supported by the National Deep Earth Science and Technology Major Project (2024ZD1003705); China Minmetals Corporation's 'Unveiling the List and Appointing the Best' Science and Technology Special Project (2025ZXA01); China Minmetals Group Youth Science and Technology Fund Project (2026QNJJA03).

Institutional review board statement: Not applicable.

Informed consent statement: Not applicable.

Data availability statement: The basic data used in this study are obtained from other

researchers, with corresponding citations in the main text.

Conflict of interest: The authors declare no conflict of interest.

AI use statement: The authors declare that no artificial intelligence (AI) tools were used in the preparation of this manuscript.

References

1. Ainalis D, Kaufmann O, Tshibangu JP, et al. Modelling the Source of Blasting for the Numerical Simulation of Blast-Induced Ground Vibrations: A Review. Rock Mechanics and Rock Engineering. 2017; 50(1): 171–193. doi: 10.1007/s00603-016-1101-2
2. Uyar GG, Aksoy CO. Comparative review and interpretation of the conventional and new methods in blast vibration. Geomechanics and Engineering. 2019; 18(5): 545–554. doi: 10.12989/GAE.2019.18.5.545
3. Jiang A, Fei H, Yan Y, et al. Cavity Effects and Prediction in the Vibration of Large-Section Rectangular Coal Roadways Induced by Deep-Hole Bench Blasting in Open-Pit Mines. Sensors. 2025; 25(11): 3393. doi: 10.3390/s25113393
4. Shi XZ, Chen X, Shi CX, et al. Prediction model for blasting-vibration-peak-speed based on GEP. Journal of Vibration and Shock. 2015; 34(10): 95–99. (in Chinese)
5. Yang J, Lu W, Li P, et al. Evaluation of Rock Vibration Generated in Blasting Excavation of Deep-buried Tunnels. KSCE Journal of Civil Engineering. 2018; 22(7): 2593–2608. doi: 10.1007/s12205-017-0240-7
6. Roy MP, Singh PK, Sarim Md, et al. Blast design and vibration control at an underground metal mine for the safety of surface structures. International Journal of Rock Mechanics and Mining Sciences. 2016; 83: 107–115. doi: 10.1016/j.ijrmms.2016.01.003
7. Shan R, Zhao Y, Wang H, et al. Blasting vibration response and safety control of mountain tunnel. Bulletin of Engineering Geology and the Environment. 2023; 82(5): 166. doi: 10.1007/s10064-023-03199-z
8. Luo Y, Gong H, Qu D, et al. Vibration velocity and frequency characteristics of surrounding rock of adjacent tunnel under blasting excavation. Scientific Reports. 2022; 12(1): 8453. doi: 10.1038/s41598-022-12203-7
9. Gou Y, Shi L, Huo X, et al. Propagation and Prediction of Blasting Vibration on Ground Surface Induced by Underground Mining with Comparison to Vibration Inside Rock. Rock Mechanics and Rock Engineering. 2024; 57(12): 10283–10306. doi: 10.1007/s00603-024-03985-5
10. Wang J, Ma B, Ning B, et al. Study on the propagation and attenuation characteristics of tunnel blasting vibration waves at different blast center distances. Journal of Applied Geophysics. 2024; 220: 105280. doi: 10.1016/j.jappgeo.2023.105280
11. Zhang J, Yan Z, Ma J, et al. Safety control of blasting vibration in new tunnel excavation adjacent to existing tunnel. Bulletin of Engineering Geology and the Environment. 2025; 84(2): 79. doi: 10.1007/s10064-025-04112-6
12. Ak H, Konuk A. The effect of discontinuity frequency on ground vibrations produced from bench blasting: A case study. Soil Dynamics and Earthquake Engineering. 2008; 28(9): 686–694. doi: 10.1016/j.soildyn.2007.11.006
13. Samareh H, Khoshrou SH, Shahriar K, et al. Optimization of a nonlinear model for predicting the ground vibration using the combinational particle swarm optimization-genetic algorithm. Journal of African Earth Sciences. 2017; 133: 36–45. doi: 10.1016/j.jafrearsci.2017.04.029
14. Armaghani DJ, Hajihassani M, Mohamad ET, et al. Blasting-induced flyrock and ground vibration prediction through an expert artificial neural network based on particle swarm optimization. Arabian Journal of Geosciences. 2014; 7(12): 5383–5396. doi: 10.1007/s12517-013-1174-0
15. Fissha Y, Khatti J, Ikeda H, et al. Predicting ground vibration during rock blasting using relevance vector machine improved with dual kernels and metaheuristic algorithms. Scientific Reports. 2024; 14(1): 20026. doi: 10.1038/s41598-024-70939-w
16. Aruna M, Vardhan H, Tripathi AK, et al. Enhancing safety in surface mine blasting operations with IoT based ground vibration monitoring and prediction system integrated with machine learning. Scientific Reports. 2025; 15(1): 3999. doi: 10.1038/s41598-025-86827-w
17. Hosseini S, Pourmirzaee R, Armaghani DJ, et al. Prediction of ground vibration due to mine blasting in a surface lead–zinc mine using machine learning ensemble techniques. Scientific Reports. 2023; 13(1): 6591. doi:

10.1038/s41598-023-33796-7
18. Zhu DP, Xie CJ, Abula T, et al. Dynamic Response Prediction of Surrounding Rock Pile under Blasting Vibration in Daqianshiling Tunnel. Chinese Journal of Underground Space and Engineering. 2021; 17(S2): 645–649. (in Chinese)
19. Zhang LG, Gong M, Yu YL. Forecast and regression analysis of blasting vibration frequency. Journal of Liaoning Technical University. 2005; (2): 187–189. (in Chinese)
20. Gao FQ, Hou AJ, Yang XL. Analysis of Blasting Vibration Duration Based on Dimension Theory. Metal Mine. 2010; 39(9): 143–145. (in Chinese)
21. Wang Q, Tao T, Jia J, et al. Analysis of blasting vibration duration considering frequency and energy and its application. Heliyon. 2024; 10(12): e33210. doi: 10.1016/j.heliyon.2024.e33210
22. Khan MFH, Hossain MJ, Ahmed MT, et al. Ground vibration effect evaluation due to blasting operations. Heliyon. 2025; 11(2): e41759. doi: 10.1016/j.heliyon.2025.e41759
23. Guan X, Xu H, Fu H, et al. Vibration characteristics, attenuation law and prediction method in the near field of tunnel blasting. Case Studies in Construction Materials. 2023; 19: e02662. doi: 10.1016/j.cscm.2023.e02662
24. Beck JL. Statistical System Identification of Structures. In: Proceedings of the 5th International Conference on Structural Safety and Reliability; 7–11 August 1989; San Francisco, CA, USA. pp. 1395–1402.
25. Hudaverdi T. Application of multivariate analysis for prediction of blast-induced ground vibrations. Soil Dynamics and Earthquake Engineering. 2012; 43: 300–308. doi: 10.1016/j.soildyn.2012.08.002
26. Wang J, Chen ZX. Robust Extreme Learning Machine Based on Truncated Maximum Correlation Entropy Criterion Loss Function. Advances in Applied Mathematics. 2023; 12(7): 3354–3364. doi: 10.12677/AAM.2023.127334 (in Chinese)